Validation of the transition state theory with Langevin-dynamics simulations

J. Schratzberger, J. Lee, M. Fuger, J. Fidler, G. Fiedler, T. Schrefl, and D. Suess

Citation: Journal of Applied Physics **108**, 033915 (2010); doi: 10.1063/1.3460639
View online: http://dx.doi.org/10.1063/1.3460639
View Table of Contents: http://scitation.aip.org/content/aip/journal/jap/108/3?ver=pdfcov
Published by the AIP Publishing

Validation of the transition state theory with Langevin-dynamics simulations

J. Schratzberger,[1] J. Lee,[1] M. Fuger,[1] J. Fidler,[1] G. Fiedler,[1] T. Schrefl,[2] and D. Suess[1,a)]
[1]*Department of Solid State Physics, Vienna University of Technology, Wiedner Hauptstrasse 8-10, 1040 Vienna, Austria*
[2]*University of Applied Science, Matthias Corvinus-Straβe 15, 3100 St. Poelten, Austria*

(Received 10 February 2010; accepted 8 June 2010; published online 11 August 2010)

Finite-element Langevin-dynamics simulations are performed in order to extract the attempt frequency of small magnetic particles as a function of an applied perpendicular field. The obtained values of the attempt frequency are in excellent agreement with the analytical results of [Kalmykov, J. Appl. Phys. **96**, 1138 (2004)]. It is shown that an external field that is applied perpendicularly to the easy axis with a strength of just about 1% of the anisotropy field is strong enough that the framework of the transition state theory (TST) for broken symmetries can be applied. It is concluded that for most realistic structures, the attempt frequency can be numerically calculated by broken symmetry—TST formulism. © *2010 American Institute of Physics*. [doi:10.1063/1.3460639]

I. INTRODUCTION

Magnetic grains in the nanoscale regime are basic constituents of various magnetic systems, ranging from magnetic recording media to biological applications. These small grains can be approximated as single-domain particles. For the case of uniaxial anisotropy and zero field, the system exhibits two equivalent ground states of opposite magnetization, which are separated by an energy barrier ΔE. According to the Néel–Brown model, the mean time τ spent in one of the states obeys an Arrhenius law

$$\tau = \tau_0 e^{\Delta E/k_B T}, \tag{1}$$

where $\tau_0^{-1} = f_0$ is the attempt frequency.

A detailed knowledge of the average lifetime of a nanomagnet is not only important for predictions of the thermal stability but also for calculating the coercive field at finite temperatures.[1,2]

Recently, various simulation techniques have been successfully applied to calculate the energy barrier numerically for magnetic structures.[3,4] However, in order to obtain a full picture for the thermal stability, a detailed knowledge of the attempt frequency is required. Based on the work of Kramers,[5] Langer,[6] and Langer and Turski,[7] the calculation of the switching rate amounts to the evaluation of the total probability current of a stationary nonequilibrium distribution through a surface near the saddle point, which can be described using the Fokker–Planck equation. Kramers derived the escape rate of point Brownian particles with separable and additive Hamiltonians from a potential well for the (i) intermediate to high damping (IHD) limit and (ii) the very low damping (VLD) limit. For all damping regimes, it was assumed that the energy barrier was much larger than the thermal energy. Kramers developed an ingenious method of treating these two damping limits but mentioned in his paper that he could not find a general method to obtain a formula that holds for any damping regime. Much later Mel'nikov and Meshkov[8] obtained an escape rate formula valid for all damping regimes what has come to be known as the Kramers turnover problem.

The paper is structured as follows: In Sec. II, we will review the results of the calculation of the attempt frequency for various damping limits and for different symmetries of the potential for a single-domain particle. In Sec. III, we will review Langer's approach for the transition state theory (TST) and apply the general multidimensional formula to derive the attempt frequency for a single-domain particle, when the external field is applied perpendicularly to the uniaxial easy axis. In Sec. IV, the analytical results are compared with finite-element Langevin dynamics simulations. A summary and outlook are given in Sec. V.

II. ATTEMPT FREQUENCY OF SINGLE-DOMAIN PARTICLE

A. Axially symmetric potential

In the case of an external field applied, $h_\parallel$, exactly parallel to the easy axis Brown[9] derived, by extending the Kramers method to spins where the Hamiltonians are in general nonseparable, the attempt frequency

$$f_0(h_\parallel) = \frac{\alpha\gamma}{1+\alpha^2}\sqrt{\frac{H_K^3}{2K_B T\pi}(1-h_\parallel)(1-h_\parallel^2)}. \tag{2}$$

Here, it is important to note that the attempt frequency depends on the volume V of the particle and the temperature T. Due to the symmetry of the magnetic system, Eq. (2) holds for all values of the damping constant (see Ref. 10 for details).

B. Broken symmetry

If the symmetry of the system is broken, the completely degenerate class of saddle points transforms to one saddle point, and the escape rate for spins now exhibits the same Kramers damping regimes as exists for point particles. Theoretical predictions of the attempt frequency for a nonaxially

a)Electronic mail: suess@magnet.atp.tuwien.ac.at.

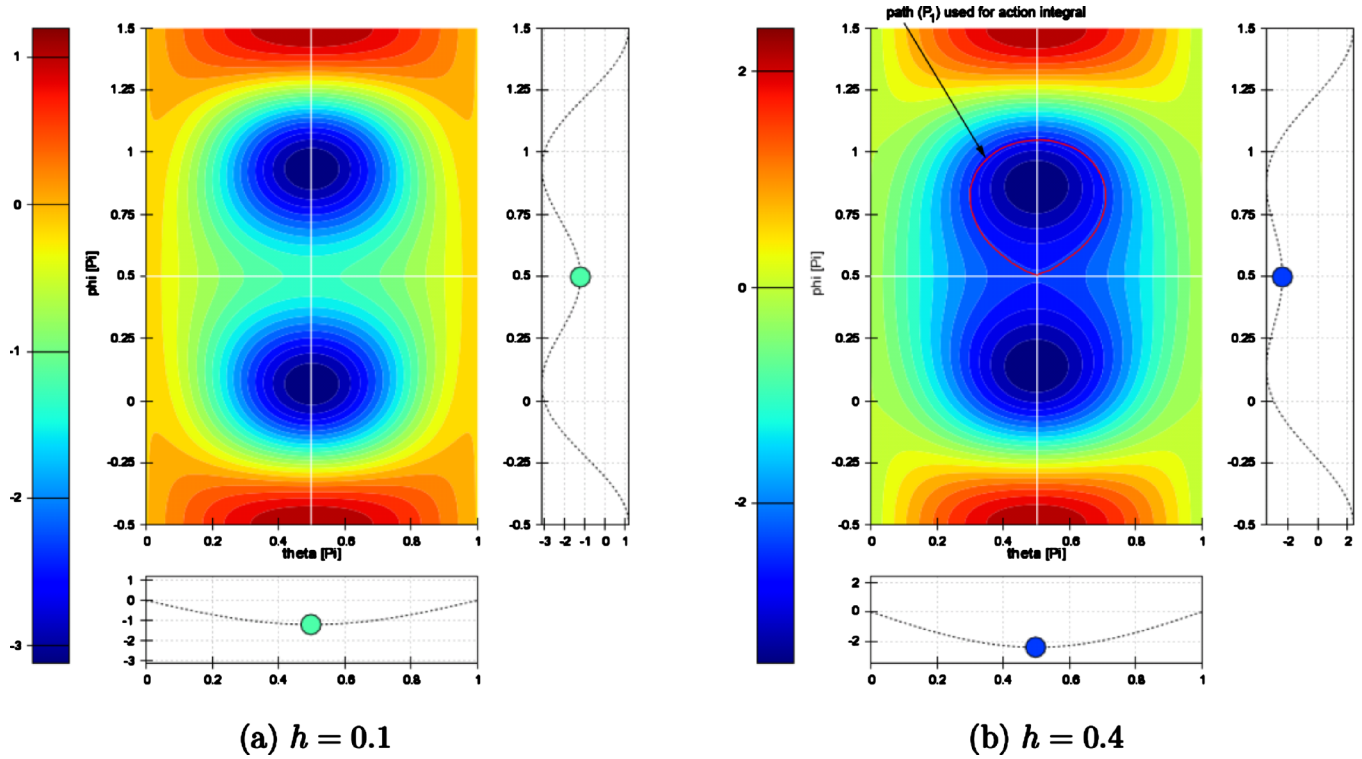

FIG. 1. (Color online) Minima and saddle point of the energy of a single-domain particle for two different values of the external field h. The path P_1 shows the path along the action S1, evaluated in Eq. (5).

symmetric potential were first derived for two limiting cases: (i) the IHD limit[11,12] and (ii) the VLD limit.[13] Coffey *et al.*[14,15] also derived in the IHD limit an explicit equation for the attempt frequency when the symmetry was broken by an external field at an angle ψ to the easy axis. Good agreement of these formulas with experimental results of single-domain particles was obtained.[15] A detailed derivation of the IHD formula for magnetic systems is given in Ref. 16. Coffey *et al.*[10] and Déjardin *et al.*[17] have also shown that the Mel'nikov–Meshkov formalism can be extended to spins in order to estimate the relaxation time for nonaxial single-domain particles for all values of the damping constant. Following Déjardin *et al.*[17] and Kalmykov,[18] the attempt frequency of a single-domain particle subjected to a magnetic field applied at an angle ψ to the easy axis for all values of the damping constant can be written as

$$f_{0,\text{general}}(h) = f_0(h)\frac{A(\alpha S_1)A(\alpha S_2)}{A(\alpha S_i + \alpha S_i)}, \tag{3}$$

where αS_i is the energy loss per cycle in well i and $f_0(h)$ is the attempt frequency in the IHD. $A(\alpha S_i)$ can be calculated by using the depopulation factor

$$A(\alpha S_i) = \exp\left[\frac{1}{\pi}\int_0^\infty \frac{\text{In}(1-\exp)[-\alpha S_i(x^2+1/4)]}{x^2+1/4}dx\right]. \tag{4}$$

For a single-domain particle, the action S_i in the well I can be calculated by evaluating the integral

$$S_i = \beta\oint_{V(\theta,\phi)=V_0}\left\{(1-\cos^2\theta)\frac{\partial}{\partial\cos\theta}V(\theta,\phi)d\phi - \frac{1}{1-\cos^2\theta}\frac{\partial}{\partial\phi}V(\theta,\phi)d(\cos\theta)\right\}. \tag{5}$$

The integral is evaluated along a path P_1 (the escape contour on one side of the saddle point) and also the escape contour along the other side of the saddle point (P_2). The energy along each path is constant and equals the saddle point energy. The path P_1 is shown in Fig. 1 by the red curve. For the case of a perpendicularly applied field, Kalmykov *et al.* approximated the action S_i by the following series:

$$S_i = 16\frac{K_1 V}{k_B T}\sqrt{h}\left[1-\frac{13}{6}h+\frac{11}{8}h^2-\frac{3}{16}h^3\cdots\right]. \tag{6}$$

The asymptotic solutions for the VLD and IHD limits have been compared with the universal formula Eq. (3) in detail by Kalmykov.[18] In Ref. 18, the validity of the universal formula in the entire damping regime is shown by comparing it with the exact solution obtained by continued fraction methods.

C. Crossover between broken symmetry and axial symmetric potentials

The nonaxially symmetric asymptotes will not reduce to the axially symmetric ones without adjustment, such as crossover formulas, which bridge the two asymptotes. This fact is stressed in the studies of diluted magnetic samples, where, due to the random anisotropy for some particles, the external field is applied almost parallel to the easy axis,

where for other particles, the symmetry is broken. In Ref. 19, it is stated that these experiments cannot be explained by using the formulas for the broken symmetry, such as in Ref. 14. The crossover problem was solved by Garanin *et al.*,[20] who developed crossover formulas between the axially-symmetric asymptotes and the asymptotes for the broken symmetry for various damping constants. The full mathematical details of the various crossover formulas can be found in Ref. 10.

III. TST FOR MULTIDIMENSIONAL SYSTEMS

The TST represents a powerful method of prediction of the rate of activated processes. Initially, in order to include fluctuations and disspipation in the TST Kramers considered in his famous paper a Brownian particle moving along the x axis, taking into account frictional and random forces imposed by the heat bath.[5] Later, Langer[6] generalized the Kramers approach to multidimensional systems, applying it to the nucleation of a multicomponent system. Although the TST was originally used for the calculation of the reaction rates for molecules, it has been shown that any system that evolves from a well-defined initial state to a final state can be treated within this framework.

Following the approach of Langer,[6] the determination of the attempt frequency amounts to calculating the total probability current of a stationary nonequilibrium distribution through a surface near the saddle point. Let us start with a system, which is described by a set of variables η_i, $i=1,\ldots,K$, which describes the K degrees of freedom of the system. In order to be able to calculate the attempt frequency, one has to know the following properties:

(i) the state $\eta_{i,\min}$ at the minimum and the state $\eta_{i,sp}$ at the saddle point,
(ii) the free energy $E(\eta_1,\ldots,\eta_k)$ at the minimum and at the saddle point, as well as the curvature of the free energy at the minimum and the saddle point,
(iii) the equation of motion, so that the dynamics of the system can be described close to the saddle point.

Knowledge of the above properties allows one to calculate the calculation of the attempt frequency, which can be written as

$$f_0 = \frac{\lambda_+}{2\pi}\Omega_0, \tag{7}$$

where λ_+ denotes for the dynamical prefactor and Ω_0 is the ratio of the well and saddle angular frequencies.

A. Calculation of λ_+

For the calculation of λ_+, one needs to know the magnetic configuration at the saddle point. The prefactor λ_+ is obtained by solving the noiseless linearized equation of motion for a configuration close to the saddle point. For a system with N spins, the noiseless equation of motion is given by the Landau–Lifshitz–Gilbert (LLG) equation as

$$\frac{\partial M_i}{\partial t} = -\gamma M \times H_{\text{eff},i} + \left(\frac{\alpha}{M_0}\right) M_i \times \frac{\partial M_i}{\partial t}, \tag{8}$$

where $\gamma = 2.210\times 10^5\ (\text{s A/m})^{-1}$ is the gyromagnetic ratio, M_i denotes the magnetization vector for the spin i in Cartesian coordinates, and V_i describes the corresponding volume of the spin i. In order to transform the system to a coordinate system that describes the $K=2N$ degrees of freedom, we rewrite the LLG equation in spherical coordinates with constant radius. Furthermore, we substitute $H_{\text{eff},i} \approx -1/\mu_0 V_i(\partial E/\partial M_i)$. We get for the LLG equations

$$f_k(\eta_1,\ldots,\eta_{2N}) = \begin{pmatrix} \frac{\partial \theta_i}{\partial t} \\ \frac{\partial \phi_i}{\partial t} \end{pmatrix} = \frac{-\gamma}{J_s V_i(1+\alpha^2)} \frac{1}{\sin\theta_i} \begin{pmatrix} \alpha \sin\theta_i \frac{\partial E}{\partial \theta_i} + \frac{\partial E}{\partial \phi_i} \\ -\frac{\partial E}{\partial \theta_i} + \frac{\alpha}{\sin\theta}\frac{\partial E}{\partial \phi_i} \end{pmatrix}, \tag{9}$$

where

$$\begin{matrix} \eta_{2i-1} = \theta_i \\ \eta_{2i} = \phi_i \end{matrix} \quad \text{and} \quad \begin{matrix} f_{2i-1}(\eta_1,\ldots,\eta_{2N}) = \frac{\partial \theta_i}{\partial t} \\ f_{2i}(\eta_1,\ldots,\eta_{2N}) = \frac{\partial \phi_i}{\partial t} \end{matrix} \tag{10}$$

and

$$E = E(\theta_1,\phi_1,\ldots,\theta_N,\phi_N) = E(\eta_1,\ldots,\eta_{2N}). \tag{11}$$

Since we need to know only the magnetization dynamics close to the saddle point, we can linearize the LLG Eq. (9) around the saddlepoint, $\bar{\eta}_k$. We get

$$\begin{pmatrix} \frac{\partial \eta_1}{\partial t} \\ \vdots \\ \frac{\partial \eta_{2N-2}}{\partial t} \end{pmatrix} \approx \begin{pmatrix} f_1(\bar{\eta}_1,\ldots,\bar{\eta}_{2N-2}) \\ \vdots \\ f_{2N-2}(\bar{\eta}_1,\ldots,\bar{\eta}_{2N-2}) \end{pmatrix} + \left. \begin{pmatrix} \frac{\partial f_1}{\partial \eta_1} & \cdots & \frac{\partial f_1}{\partial \eta_{2N-2}} \\ \vdots & \ddots & \vdots \\ \frac{\partial f_{2N-2}}{\partial \eta_1} & \cdots & \frac{\partial f_{2N-2}}{\partial \eta_{2N-2}} \end{pmatrix} \right|_{SP} \times \begin{pmatrix} \eta_1 - \bar{\eta}_1 \\ \vdots \\ \eta_{2N-2} - \bar{\eta}_{2N-2} \end{pmatrix}, \tag{12}$$

where $f_k = f_k(\eta_1,\ldots,\eta_{2N-2})$ and $(\eta_k - \bar{\eta}_k = \nu_k)$. At the saddle point of the energy, $f_k(\bar{\eta}_1,\ldots,\bar{\eta}_{2N-2})$ vanishes. Hence, we rewrite the equation above and get

$$\begin{pmatrix} \frac{\partial v_1}{\partial t} \\ \vdots \\ \frac{\partial v_{2N-2}}{\partial t} \end{pmatrix} \approx H_{\mathrm{dyn}} \begin{pmatrix} v_1 \\ \vdots \\ v_{2N-2} \end{pmatrix}, \tag{13}$$

where

$$H_{\mathrm{dyn}} = \left. \begin{pmatrix} \frac{\partial f_1}{\partial \eta_1} & \cdots & \frac{\partial f_1}{\partial \eta_{2N-2}} \\ \vdots & \ddots & \vdots \\ \frac{\partial f_{2N-2}}{\partial \eta_1} & \cdots & \frac{\partial f_{2N-2}}{\partial \eta_{2N-2}} \end{pmatrix} \right|_{SP}. \tag{14}$$

The solution of the dynamics close to the saddle point leads to the ansatz

$$\vec{\nu} = \vec{\nu}^0 e^{\lambda t}, \tag{15}$$

which describes the exponential change in the magnetic configuration close to the saddle point. By inserting the ansatz (15) into (13), we get

$$\lambda \vec{\nu}^0 = H_{\mathrm{dyn}} \vec{\nu}^0. \tag{16}$$

Due to the construction of the matrix H_{dyn} the eigenvalue problem according to Eq. (16) has only one positive eigenvalue. This positive eigenvalue is λ_+ of Eq. (7). Hence, the problem of calculating λ_+, which is required to evaluate Eq. (7) reduces to the determination of the positive eigenvalue of the matrix H_{dyn}.

B. Calculation of Ω_0

Ω_0 is obtained by evaluating the curvature of the free energy E at the saddle point and at the minimum. The curvature is obtained by calculating the second derivative of the energy.

$$H_{\mathrm{stat}} = \begin{pmatrix} \frac{\partial h_1}{\partial \eta_1} & \cdots & \frac{\partial h_1}{\partial \eta_{2N-2}} \\ \vdots & \ddots & \vdots \\ \frac{\partial h_{2N-2}}{\partial \eta_1} & \cdots & \frac{\partial h_{2N-2}}{\partial \eta_{2N-2}} \end{pmatrix} = \begin{pmatrix} \frac{\partial^2 E}{\partial \eta_1 \partial \eta_1} & \cdots & \frac{\partial^2 E}{\partial \eta_{2N-2} \partial \eta_1} \\ \vdots & \ddots & \vdots \\ \frac{\partial^2 E}{\partial \eta_1 \partial \eta_{2N-2}} & \cdots & \frac{\partial^2 E}{\partial \eta_{2N-2} \partial \eta_{2N-2}} \end{pmatrix}, \tag{17}$$

where $h_k(\eta_1, \ldots, \eta_{2N-2}) = (\partial E / \partial \eta_k)$. The ratio Ω_0 in Eq. (7) is obtained by calculating the determinant of the matrix H_{stat} as

$$\Omega_0 = \sqrt{\frac{\det(H_{\mathrm{stat}})|_{\min}}{-\det(H_{\mathrm{stat}})|_{sp}}} \tag{18}$$

From Eqs. (16) and (18), the attempt frequency can be calculated using Eq. (7). We emphasize that these formulas are valid only in the IHD. In order to generalize them to any value of the damping constant, the formalism resulting in Eq. (3) can be applied.

C. Example: single-domain particle with external field perpendicular to easy axis

In this section, we will apply the previous results in order to calculate the attempt frequency of a single-domain particle, where the external field is applied perpendicularly to the uniaxial easy axis. In Ref. 21, a similar derivation is performed under the assumption of a hard axis anisotropy perpendicular to the easy axis. The total energy of a magnetic particle can be described by the theory of micromagnetics as

$$E = \int \{A(\nabla \mathbf{u})^2 - K_E(\hat{\mathbf{e}}_{\mathrm{easy}} \cdot \mathbf{u})^2 - \mathbf{J} \cdot \mathbf{H}_{\mathrm{ext}} - \mathbf{J} \cdot \mathbf{H}_{\mathrm{demag}}\} dV, \tag{19}$$

where $J_S[\mathrm{T}]$ is the magnetization polarization, $K_e[\mathrm{J/m^3}]$ is the crystalline anisotropy constant, and $A[\mathrm{J/m}]$ is the exchange constant. For a magnetic particle whose dimensions are smaller than the domain wall width, we assume that the magnetization remains homogeneous within the particle. Hence, we will neglect the first term in Eq. (19). If we assume a spherical particle, we can also neglect the last term in Eq. (19). In the following, we assume that $\hat{\mathbf{e}}_{\mathrm{easy}}$ points in the x-direction and the external field $\mathbf{H}_{\mathrm{ext}}$ points in the y-direction. Introducing polar coordinates ($u_x = \sin\vartheta \cos\varphi$, $u_y = \sin\vartheta \sin\varphi$, and $u_z = \sin\vartheta$), we get,

$$E = -VK_E(\sin^2\vartheta \cos^2\varphi + 2h_\perp \sin\vartheta \sin\varphi), \tag{20}$$

with

$$h_\perp = \frac{H_y J_s}{2K_E}. \tag{21}$$

The two minima of the energy are situated at $\theta_{\min,1} = \pi/2$, $\phi_{\min,1} = \arcsin(h)$ and $\theta_{\min,2} = \pi/2$, $\phi_{\min,1} = \pi - \arcsin(h)$. The saddle point configuration is $\theta_{sp} = \phi_{sp} = \pi/2$. The contour plot of the energy for two different values of the external field h is shown in Fig. 1.

Substituting Eq. (20) into Eq. (17), we get at the minimum

$$H_{\mathrm{stat,min}} = \begin{bmatrix} 2h^2 VK_e + 2(1-h^2)VK_e & 0 \\ 0 & 2(1-h^2)VK_e \end{bmatrix}, \tag{22}$$

and at the maximum

$$H_{\mathrm{stat},sp} = \begin{bmatrix} 2hVK_e & 0 \\ 0 & (h-1)2VK_e \end{bmatrix} \tag{23}$$

Using Eq. (22) and Eq. (23) for the evaluation of Eq. (18), we get for the statical prefactor $\Omega_0 = \sqrt{1+1/h}$.

Substituting Eq. (20) into Eq. (9) and Eq. (23), we can calculate the dynamical prefactor, which leads together with the static prefactor to the attempt frequency in the IHD:

$$f_0 = \frac{1}{2\pi}\lambda_+\Omega_0 = \frac{1}{2\pi}\left[\frac{\gamma_1 K_e}{J_s(1+\alpha^2)}(\alpha(1-2h) + \sqrt{\alpha^2 - 4h(h-1)})\right]\sqrt{1+\frac{1}{h}}, \quad (24)$$

which agrees with the results obtained by Coffey *et al.*,[14] which was derived as a special case of the Langer theory.

IV. COMPARING TST WITH LANGEVIN-DYNAMICS SIMULATIONS

As mentioned in Sec. II, the formulas for the attempt frequency for the broken symmetry and the axial symmetric case do not converge to each other when the external field $h \rightarrow 0$ without additional adjustment.[20] In order to judge the applicability of the formula for the broken symmetry [Eq. (24)] and the formula for the axial symmetric case [Eq. (2)], we perform micromagnetic simulation using Langevin-dynamics, where we adjust the broken symmetry by applying perpendicularly applied fields $h = H_{ext}/H_{ani}$ with different amplitudes. In real magnetic structures, it seems reasonable that due to imperfections, in most cases the symmetry is broken to a certain degree. A detailed discussion about the requirements for the application of the formulas for broken symmetry, in order to explain experimental results, can be found in Ref. 19.

Recently, various groups have claimed good agreement between Langevin-dynamics simulations and analytical expressions for the attempt frequency for various damping limits.[22–24] Usov and Grebenshchikov[24] compared the relaxation time of a single-domain particle with a nonaxially symmetric double-well potential with Langevin-dynamics simulations and found good agreement of the magnetization relaxation process. Vouille *et al.*[22] compared Langevin-dynamics simulations with the formulas of Ref. 15 and found favorable agreement with Coffey's formulae. Suh *et al.*[23] have shown that there is an excellent agreement between the attempt frequency obtained from Langevin-dynamics simulations and the theoretical formulas of the attempt frequency [Eqs. (2) and (3)] for nanomagnets with thin-film geometry. In Refs. 22–24, the Langevin-dynamics simulations were performed in the macrospin approximation, where the nanomagnet was represented by one magnetization vector only. In the following Langevin-dynamics simulations, the magnet is subdivided into several finite elements in order to resolve magnetization inhomogeneities. The mesh size dependence is minimized by using a scaling approach.[25]

To study the average lifetime of a single particle, a series of simulations are performed, where the particle's magnetization along the easy axis is measured as a function of time. Thus, the mean life time τ of Eq. (1) becomes directly accessible. This type of measurement is called telegraph noise measurement because of the expected stochastic fluctuation between the two states of lowest energy (see Fig. 2). As τ increases exponentially with decreasing temperature, it is very unlikely that an escape process will be observed at low temperatures. However, applying a constant field perpendicularly to the easy axis reduces the height of the energy barrier. When the energy barrier is sufficiently small, enough

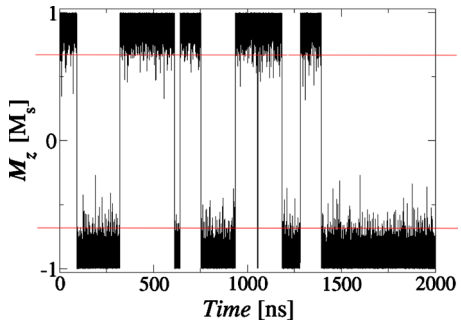

FIG. 2. (Color online) The time evolution of the magnetization at finite temperature is shown. The input parameters are as follows: $h=0.2$, cube length a=1.0 nm, T=18 K, $J_S=0.5$ T, $K_E=3\times10^6$ J/m^3, and $\alpha=0.05$. The number of finite elements to discretize the cube is 13.

switching events will occur in order to obtain τ with a reasonable accuracy. In order to extract τ_0 from τ, we perform various simulations. The magnetic properties are compiled in the caption of Fig. 2. In order to be able to calculate the average lifetime of a particle, it is essential to define the switching event properly. In the following simulations, we defined a particle to be switched when both of the following criteria apply: (i) the z-component of the magnetization (component parallel to easy axis) has to overcome a threshold of $m_z/m_s = \pm 0.87$ and (ii) the magnetization has to perform at least one full precessional cycle around the minimum of the switched state.[26] In order to estimate the attempt frequency if τ is measured, Eq. (1) is used. In order to be able to obtain accurate fits, we use only $\tau_0 = 1/f_0$ as a fit parameter. The energy barrier E_0 is obtained from the simulation using the nudged elastic band method.[3]

In the first simulation, we studied the influence of the discretization size on the attempt frequency. Figure 3 shows

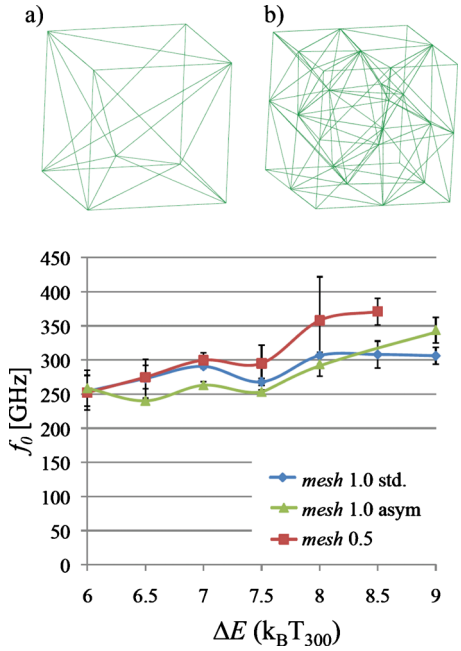

FIG. 3. (Color online) Results of a cube with for different finite element mesh sizes; the other parameters are the same as in Fig. 2. (a) mesh size =1.0 nm and (b) mesh size=0.5 nm.

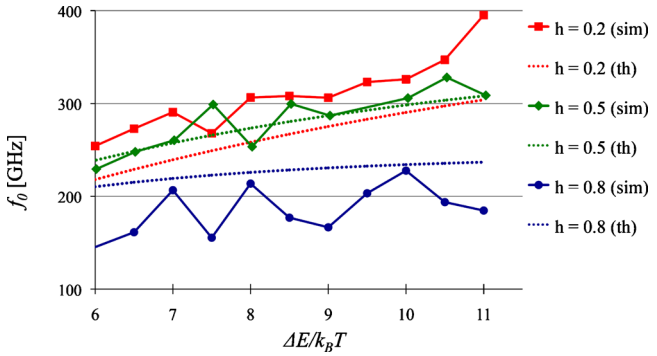

FIG. 4. (Color online) Attempt frequency as a function of the temperature. The magnetic parameters are the same as in Fig. 2. The dotted lines are analytical results according to Eq. (3), using the approximation of Eq. (6).

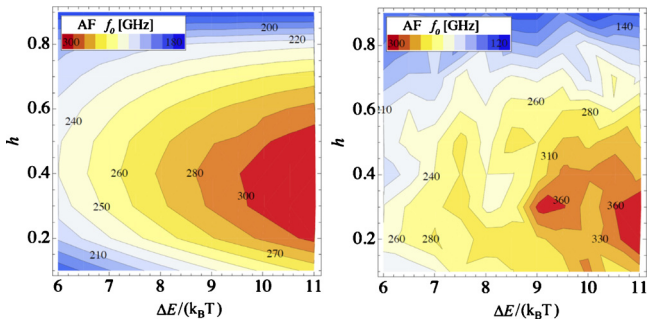

FIG. 6. (Color online) Contour plot of the attempt frequency as a function of temperature and external field h. (left) f_0 according to Eq. (24). (right) f_0 obtained by Langevin-dynamics simulations. The magnetic parameters are the same as in Fig. 2.

a weak dependence of f_0 on the mesh size. In all of the following simulations, a mesh size of 1 nm was assumed, which leads to 13 finite elements.

Figure 4 shows the attempt frequency as a function of temperature for different values of the applied perpendicular field. According to Eq. (24), the attempt frequency does not depend on temperature in the IHD. However, the Langevin simulations clearly show an increase in f_0 as function of 1/T. The results of the Langevin simulations are clearly supported by extending the analytical simulation to the general equation, which is valid for all values of the damping constant. In the comparison, we evaluate f_0 with Eq. (3) and use the approximation of Eq. (6).

The dependence of the attempt frequency as a function of the external field is shown in detail in Fig. 5. Again, the Langevin simulations are compared with analytical results. The analytical formula for the IHD for the broken symmetries Eq. (24) clearly overestimates the attempt frequency. In the limit when the external field approaches zero, the attempt frequency obtained by Langevin dynamics simulations converge to a value, which is also smaller than the prediction of Eq. (2). Again, the general equation Eq. (3) for the attempt frequency, which is valid for all values of the damping constant, describes the simulation results very well. Although the analytical formula Eq. (24) diverges for $h \to 0$, which one must remember is an artifact[10,20] of the steepest descents

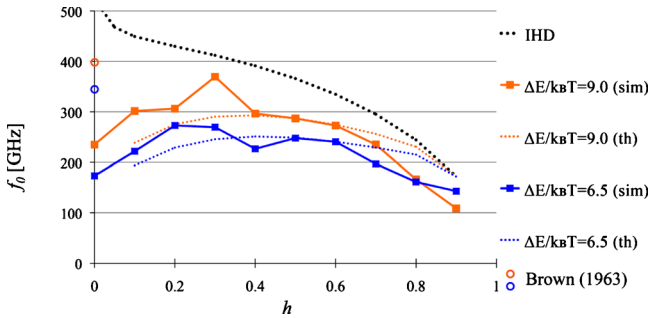

FIG. 5. (Color online) Attempt frequency as a function of the perpendicular external field strength. The magnetic parameters are the same as in Fig. 2. (IHD) is the analytical results in the intermediate to high damping limit according to Eq. (24) (Ref. 9). is the analytical result for the symmetric case according to Eq. (2). The two dotted lines at the bottom (blue and red) are analytical results, valid for all damping values according to Eq. (3) using the approximation of Eq. (6)

approximation used to evaluate the various integrals, the general equation for the attempt frequency [Eq. (3)] seems to converge to a finite value. The comparison between Eq. (3) and the results of f_0 obtained by Langevin dynamics simulations are summarized by the contour plot of Fig. 6. Although sharp contours require a large amount of simulation points, the overall agreement can be seen well.

V. CONCLUSION AND OUTLOOK

Langevin-dynamics simulations of the single-domain particle confirm the validity of Eq. (3). The broken symmetry cases seem to be relevant for all realistic samples studied in this paper. As a consequence, the formalism summarized in Eqs. (7)–(18) seems to be a useful framework to estimate the thermal stability for large magnetic structures, including arbitrary shaped geometries and inhomogeneous magnetization configurations. This will allow us to estimate the long-term thermal stability of magnetic structures that cannot be accessed by Langevin-dynamics simulations. The attempt frequency in the IHD limit can be calculated numerically if: (i) the second derivative of the energy at the saddle point and at the minimum is known and (ii) the magnetization dynamics around the saddle point can be expressed as shown in Eq. (12). All of these properties are usually accessible in micromagnetic simulations, which will allow for the calculation of the attempt frequency in the IHD limit. Starting from this approximation, correction to the general formula, which is valid for all values of the damping constant, can be tackled numerically. A promising route will be to investigate the energy loss per cycle in both wells next to the saddle point.

ACKNOWLEDGMENTS

The financial support of the FWF Projects No. P20306, No. F4112-N13, and the support of the European Project TERAMAGSTOR (Grant No. FP7-ITC-2007-2-224001) are acknowledged.

[1]R. W. Chantrell, N. Walmsley, J. Gore, and M. Maylin, Phys. Rev. B **63**, 024410 (2000).
[2]M. P. Sharrock, J. Appl. Phys. **76**, 6413 (1994).
[3]R. Dittrich, T. Schrefl, D. Suess, W. Scholz, H. Forster, and J. Fidler, J. Magn. Magn. Mater. **250**, 12 (2002).
[4]E. Paz, F. Garcia-Sanchez, and O. Chubykalo-Fesenko, Physica B **403**, 330 (2008).

[5]H. A. Kramers, Physica (Utrecht) **7**, 284 (1940).
[6]J. S. Langer, Ann. Phys. (N.Y.) **41**, 108 (1967).
[7]J. S. Langer and L. A. Turski, Phys. Rev. A **8**, 3230 (1973).
[8]V. I. Mel'nikov and S. V. Meshkov, J. Chem. Phys. **85**, 1018 (1986).
[9]W. F. Brown, Phys. Rev. **130**, 1677 (1963).
[10]W. T. Coffey, D. A. Garanin, and D. McCarthy, Adv. Chem. Phys. **117**, 483 (2001).
[11]D. A. Smith and F. A. de Rozario, J. Magn. Magn. Mater. **3**, 219 (1976).
[12]W. F. Brown, IEEE Trans. Magn. **15**, 1196 (1979).
[13]I. Klik and L. Gunther, J. Stat. Phys. **60**, 473 (1990).
[14]W. T. Coffey, D. S. F. Crothers, J. L. Dormann, L. J. Geoghegan, and E. C. Kennedy, Phys. Rev. B **58**, 3249 (1998).
[15]W. T. Coffey, D. S. F. Crothers, J. L. Dormann, Y. P. Kalmykov, E. C. Kennedy, and W. Wernsdorfer, Phys. Rev. Lett. **80**, 5655 (1998).
[16]L. J. Geoghegan, W. T. Coffey, and B. Mulligan, Adv. Chem. Phys. **100**, 475 (1997).
[17]P. M. Déjardin, D. S. F. Crothers, W. T. Coffey, and D. J. McCarthy, Phys. Rev. E **63**, 021102 (2001).
[18]Y. P. Kalmykov, J. Appl. Phys. **96**, 1138 (2004).
[19]H. Kachkachi, W. T. Coffey, D. S. F. Crothers, A. Ezzir, E. C. Kennedy, M. Noguès, and E. Tronc, J. Phys.: Condens. Matter **3077**, 12 (2000).
[20]D. A. Garanin, E. C. Kennedy, D. S. F. Crothers, and W. T. Coffey, Phys. Rev. E **60**, 6499 (1999).
[21]H. B. Braun, J. Appl. Phys. **76**, 15 (1994).
[22]C. Vouille, A. Thiaville, and J. Miltat, J. Magn. Magn. Mater. **272–276**, E1237 (2004).
[23]H.-J. Suh, C. Heo, C.-Y. You, W. Kim, T.-D. Lee, and K.-J. Lee, Phys. Rev. B **78**, 064430 (2008).
[24]N. A. Usov and Y. B. Grebenshchikov, J. Appl. Phys. **105**, 043904 (2009).
[25]M. Kirschner, T. Schrefl, F. Dorfbauer, G. Hrkac, D. Suess, and J. Fidler, J. Appl. Phys. **97**, 10E301 (2005).
[26]S. Wang and P. B. Visscher, J. Appl. Phys. **99**, 08G106 (2006).